EVAPORATION OF LIQUID HYDROCARBONS IN HEATED CLOSED CONTAINERS

V. V. Malyshev and E. P. Zlobin

UDC 536.423.1:661.715/.716

Results are shown of a study concerning the evaporation of liquid hydrocarbons in externally heated closed containers.

The processes of heat and mass transfer which occur in closed containers during changes in the temperature do, to a large measure, determine the conditions under which petroleum products are stored. Natural convection in metallic containers with petroleum was studied in [1]. In this article we show the results of a study concerning the mass transfer processes within the vapor–air space in closed containers which occur when petroleum products evaporate under quasisteady thermal conditions.

The procedure in this study included the use of a Tepler shadowgraph. The test apparatus is shown in Fig. 1. It consisted of a model IAB-451 Tepler instrument 1, a thermostat 2, and the test container 3 in the form of a double-wall cylindrical vessel made of aluminum alloy 200 mm long and 144 mm in diameter inside, with glass windows in the end planes. Into the inner cylinder cavity was poured liquid isooctane. Through the gap space between walls was circulated a liquid heat carrier (water), entering from the thermostat at the bottom and leaving from a receptacle at the top back into the thermostat. Six thermocouples 4 were suspended through the drain tube on top, for measuring and recording the temperature throughout the experiment.

The shadowgraph was provided with a linear color raster, a frame with a grid of narrow (0.7-0.8 mm wide) transparent color strips, mounted between two parallel optical glasses. When a light beam passed through the cylindrical cavity containing an optically homogeneous medium (no density gradient), it also passed then through the focus of the receiver optics and appeared in the same color as the strip through which it had passed. In this case one homogeneous image of the same color appeared on the shadowgraph

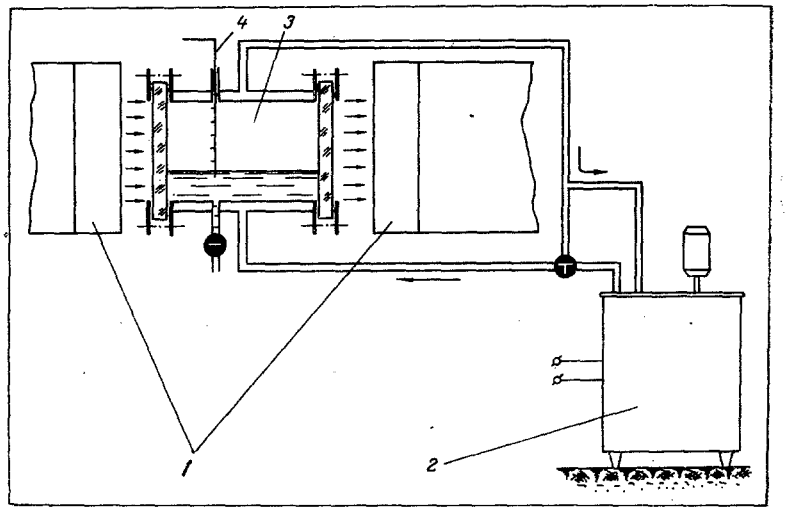

Fig. 1. Schematic diagram of the test apparatus.

Translated from Inzhenerno-Fizicheskii Zhurnal, Vol. 23, No. 4, pp. 701-708, October, 1972. Original article submitted April 29, 1972.

screen covering the entire field. With an optical inhomogeneity in any part of the container, the light beam passing through it was deflected from the focus by an angle depending on the particular change in the refractive index. The thus deflected light beam then passed through a different raster strip and on the shadowgraph screen appeared a spot in the color corresponding to that strip.

The width of each color strip on the raster strip and the spacing of strips across the raster were measured (on a dial, with the aid of a micrometer screw on the shadowgraph) before the experiment had started. The shadowgraph was adjusted to any one particular color strip on the raster.

A definite quantity of isooctane was poured into the container. It was then heated at a predetermined rate. The images of emerging inhomogeneities, characterizing the dynamics of mass transfer inside the container, were photographed at definite time intervals. The temperature inside the container was, at the same time, continuously recorded. The pressure inside the container was maintained at atmospheric level throughout the experiment. An evaluation of the test results had thus been reduced to an interpretation of photographs.

Each photograph may be considered representing a container section perpendicular to the container axis, with the inhomogeneity represented by areas of different colors. Regions of the vapor–air space appeared as strips parallel to the liquid surface in the container. With the spacing between the color strips of the raster (their coordinates referred to one another) known, one could determine the deflection angles of the light beam over the entire container section $\varepsilon = \Delta/f$.

Inasmuch as the path length of a light beam through the container was known (distance between the inner surfaces of the glass windows), the refractive-index gradient was

$$\frac{dn}{dy} = \frac{n_0}{l}\varepsilon.$$

Such an analysis of the photographs yielded an empirical formula for the refractive-index gradient along the height of the vapor–air space at the time each frame was taken.

It is to be noted that regions with the same refractive-index gradient were very stable even under a high heating rate (8-10°C/min). During fluctuations in the plane perpendicular to the container axis, the oscillations of these regions followed the oscillations of the isooctane surface. It seemed as if immiscible liquids of different colors and densities oscillated. In studying the dynamics of mass transfer within the vapor–air space, we have not detected any manifestations of one phase penetrating into another, which would usually occur during convection within a volume of heated isooctane.

In some tests we also tried to establish the existence of transverse gradients (in the direction parallel to the free surface of the liquid and to the planes of the windows), but none was detected.

Under such conditions, therefore, mass transfer within the vapor–air space of the container was determined basically by the law of molecular diffusion with an additional Stefan flux due to the phase change during evaporation.

Deriving the equation of mass transfer for our test conditions is analogous to deriving the equation of heat conduction [2] with the specific relation between thermal conductivity and diffusivity taken into account [3]. Only a concentration gradient along the y-axis, perpendicular to the free surface of the liquid, is assumed in the derivation. Considering the geometry of the space where mass transfer occurs, we have the following equation:

$$\frac{dk}{d\tau} - D\left[\frac{\partial^2 k}{\partial y^2} + \frac{\partial k}{\partial y}\cdot\frac{D' - 2y}{2y(D' - y)}\right] = 0. \tag{1}$$

Since a concentration gradient exists only along the y-axis, hence

$$\frac{dk}{d\tau} = \frac{\partial k}{\partial \tau} + w_y\frac{\partial k}{\partial y}. \tag{2}$$

Inserting (2) into (1) yields

$$\frac{\partial k}{\partial \tau} + w_y\frac{\partial k}{\partial y} - D\frac{\partial^2 k}{\partial y^2} - D\frac{\partial k}{\partial y}\cdot\frac{D' - 2y}{2y(D' - y)} = 0. \tag{3}$$

Unlike the classical equation of molecular diffusion, this one includes a so-called Stefan term (second term) and a term accounting for the geometry of the container space (fourth term). According to Fick's law

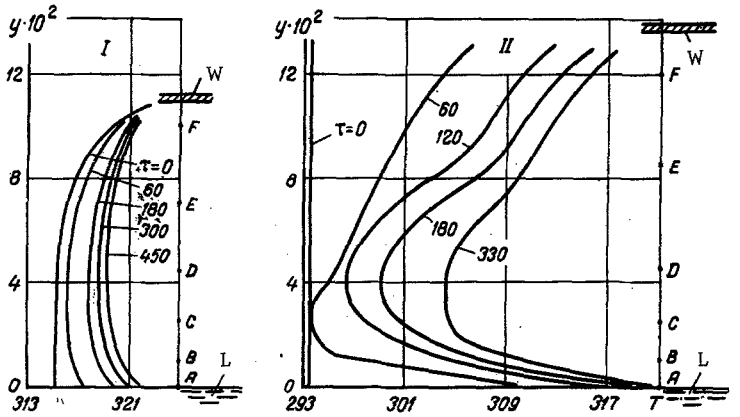

Fig. 2. Temperature profile T (°K) along the container height y (m), at various instants of time τ (sec) (A, B, C, D, E, F are the locations of thermocouples along the container height; W indicates the location of the upper container wall; L indicates the location of the liquid phase): I) "moderate" heating; II) "rapid" heating.

with the Stefan correction [3] and a correction for the container geometry, we have

$$w_y = -\frac{D}{1-(k)_{y_0}}\left(\frac{\partial k}{\partial y}\right)_{y_0}\sqrt{\frac{y_0(D-y_0)}{y(D-y)}}. \qquad (4)$$

The minus sign indicates that the positive direction of w_y is opposite to the direction of gradient $\partial k/\partial y$.

Inserting (4) into (3) yields

$$\frac{\partial k}{\partial \tau} = D\left[\frac{\partial^2 k}{\partial y^2} + \frac{1}{1-(k)_{y_0}}\left(\frac{\partial k}{\partial y}\right)_{y_0}\sqrt{\frac{y_0(D-y_0)}{y(D-y)}}\frac{\partial k}{\partial y} + \frac{D-2y}{2y(D-y)}\cdot\frac{\partial k}{\partial y}\right].$$

All numerical calculations, including those for Eq. (5), were made on a BÉSM-4 computer. As a result we have established the relation $k = k(y, \tau)$.

With a relation $T = T(y, \tau)$ based on tests available, $\rho = \rho(y, \tau)$ was calculated by the formula

$$\rho = \frac{P\left[kR_A + (1-k)R_H\right]}{TR_AR_H\gamma}.$$

Further calculations included $\bar{\mu} = \bar{\mu}(y, \tau)$ by the formula

$$\bar{\mu} = \mu_H k + \mu_A(1-k),$$

$\bar{r} = \bar{r}(y, \tau)$ by the formula

$$\bar{r} = r_H k + r_A(1-k),$$

$n = n(y, \tau)$ by the formula

$$\bar{r} = \left(\frac{n^2-1}{n^2-2}\right)\frac{\bar{\mu}}{\rho}$$

and, finally,

$$\operatorname{grad} n = \operatorname{grad} n(y, \tau).$$

Values of the thermophysical properties were taken from [4].

Results based on two experiments with different heating rates are shown in Figs. 2 and 3. The temperature profiles along the height of the vapor–air space are shown in Fig. 3 at several different instants of time during these experiments. According to the graphs, the temperature rise in the liquid phase within the first 60 sec was 2°K during "moderate" heating and 16°K during "rapid" heating.

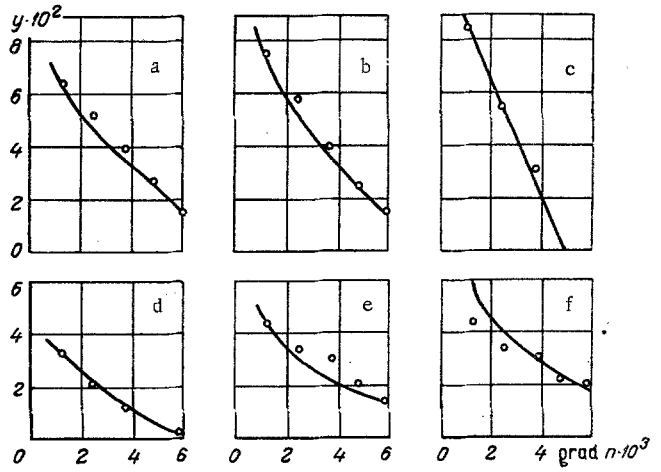

Fig. 3. Refractive-index gradient grad n (m^{-1}) as a function of the height in the container y (m), at various instants of time τ (sec): a) "moderate" heating at $\tau = 0$ sec; b) 60 sec; c) 300 sec; d) "rapid" heating at $\tau = 0$ sec; e) 60 sec; f) 120 sec. Curves represent calculated relations, points represent test points.

The refractive-index gradient along the height of the vapor–air space is shown in Fig. 3 at various instants of time.

Some discrepancy between test data and calculations, especially in the case of "rapid" heating (8-10°C/min) can be explained by a convective mass transfer, in addition to the diffusive mass transfer, at the lateral container surface as a result of the large temperature difference (especially during the first few minutes of heating) between the container wall and the vapor–air medium inside it. For this reason, although this temperature difference diminished fast with time, the vapor concentration in the upper region of the container was somewhat higher than calculated (curve K_E in Fig. 4) on the basis of diffusive mass transfer alone (curve K_C in Fig. 4).

The inner space generally and the vapor–air region in particular were heated through the walls and, therefore, the temperature was higher directly at the wall than inside the container. Since the temperature of the liquid phase rose continuously, hence the vapor concentration at the interphase boundary in the

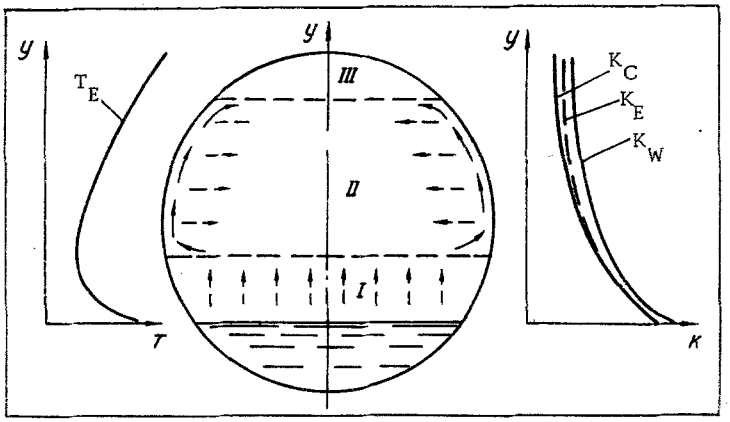

Fig. 4. Model of the heat and mass transfer in the test container. I, II, III) characteristic zones of heat and mass transfer under the test conditions are (solid arrows indicate convective currents, dashed arrows indicate diffusive currents): T_E) temperature profile along the container height; K_W, K_E) true profiles of vapor concentration along the container height at the wall and father away from the wall, respectively; K_C) calculated concentration profile farther away from the wall without convection at the wall.

vapor–air space also increased and throughout the heating period remained higher than in the rest of the space. According to calculations with the empirical relation $T = T(y, \tau)$ taken into account, the concentration of isooctane vapor and the density of the vapor–air mixture decreased away from the free surface of the liquid.

For an arbitrary horizontal container segment, we will analyze the parameters of the air–vapor mixture in the immediate vicinity of the wall surface and farther away from it. We assume that no convective motion due to Archimedes forces occurred at the lateral wall, even though the temperature was higher directly at the wall than further away from it. The correctness of this assumption was confirmed by tests. This means that the density of the vapor–air mixture in this segment was the same at the wall and farther away from it.

Such a condition, when there is a temperature difference, must be due to a corresponding difference between the vapor concentration at the wall and farther away from it. Considering that the density of isooctane is much higher than that of air (approximately four times), the vapor concentration distribution should be analogous to the vapor temperature distribution over a given segment, i.e., a higher vapor concentration should correspond to a higher vapor temperature. The profile of vapor concentration along the container height should correspond to curves K_W and K_E in Fig. 4.

Let the temperature of the wall rise somewhat within a certain interval of heating time. The boundary layer, being nearest to the heated wall, will heat up faster than the layer at the container axis and its density will become lower. The Archimedes force acting on the vapor–air volume of the boundary layer within the given segment will lift it upward through some distance Δy. As a result, two different situations may prevail in the horizontal segment located at the height Δy above the original one:

1) the density of the lifted vapor–air layer (warmer and with a higher vapor concentration) becomes equal to that of the vapor–air mixture farther away from the wall: the motion ceases;

2) the density of the lifted vapor–air layer remains lower than the density farther away from the wall: the motion continues.

The first of these situations occurs within the zone of high vapor concentration gradients along the container height, the second of these situations is most likely to occur within the zones of very small such gradients.

Thus, in the vapor–air space of the heated container one can distinguish the following different zones of mass transfer (Fig. 4).

Zone I directly above the liquid, with almost no convection due to Archimedes forces, is characterized by appreciable gradients of vapor concentration.

Zone II above zone I, with significant convection at the wall, is characterized by very small vapor concentration gradients along the container height.

Zone III above zone II and extending to the top wall, with conductive heat and mass transfer, is characterized by the maximum temperature and the minimum concentration, i.e., by the minimum density.

The widths of zones I and II depend on the concentration gradient, on the heating rate, and on the ratio of the molecular weights of vapor and air, while the width of zone III depends mainly on the heating mode. Inasmuch as zone III is characterized by the accumulation of hottest and lightest masses, it will expand due to external heating through the wall as well as due to hot currents entering it from zone II by convection.

An analysis of the vapor concentration gradient along the container height leads to the conclusion that the convectionless zone II adjoining the liquid resists the spreading of the hydrocarbon vapor concentration. One may consider the free surface of the liquid as the "input" terminal of this resistance and the interzone I-II boundary as its "output" terminal. Convective currents at the wall are capable to carry a vapor–air mass with a very definite and limited level of high vapor concentration. This level is determined by the heating rate and by the ratio of molecular weights of vapor and air. The region of high vapor concentration is the interface between zones I and II. The proposed model of mass transfer inside a closed container is shown in Fig. 4.

In order to answer some questions raised here, additional studies were made on the basis of another principle.

A thin-walled container with some amount of liquid hydrocarbon (isooctane or decane) was heated in a thermostat. The vapor–air mixture was passed from this vessel through a refrigerator, where it was purged of vapor, and fed into a measuring vessel. Test data on the rate of air intake, characterized by both thermal expansion and evaporation, agreed fairly well with calculations. The calculations were based on formulas analogous to those described earlier, also with the assumption that evaporation occurs by diffusion. This again confirms the results of our test results obtained by the shadowgraph method.

NOTATION

ε	is the angle of light-beam deflection;
Δ	is the distance from the raster strip to which the Tepler instrument was tuned (with $\varepsilon = 0$);
f	is the focal length of the Tepler instrument;
n	is the instantaneous refractive index in the container;
n_0	is the refractive index in the container under normal conditions;
y	is the linear coordinate perpendicular to the liquid level;
l	is the path length of the light beam through the container;
k	is the vapor concentration;
τ	is the time coordinate;
w_y	is the Stefan velocity;
D	is the vapor diffusivity in air;
D'	is the diameter of the container;
y_0	is the coordinate of the liquid level;
T	is the temperature;
ρ	is the referred density of the vapor–air mixture;
γ	is the density of water at 4°C;
P	is the pressure inside the container;
R_A, R_H	are the gas constants of air and hydrocarbon vapor, respectively;
$\bar{\mu}$, μ_A, μ_H	are the molecular weights of the mixture, of air, and of hydrocarbon vapor, respectively;
$\bar{r}$, r_A, r_H	are the molecular refractions of the mixture, of air, and of hydrocarbon vapor, respectively;
$k(y, \tau)$	denotes k as a function of y, τ;
grad n	is the refractive index gradient.

Subscripts

y_0 denotes the value at $y = y_0$.

LITERATURE CITED

1. K. V. Elshin, Inzh.-Fiz. Zh., No. 9 (1959).
2. M. A. Mikheev, Fundamentals of Heat Transmission [in Russian], Gosenergoizdat, Moscow (1956).
3. A. V. Lykov, Heat and Mass Transfer in Desiccation Processes [in Russian], Gosenergoizdat, Moscow (1956).
4. S. S. Kutateladze and V. M. Borishanskii, Handbook on Heat Transmission [in Russian], Gosenergoizdat, Moscow (1959).
5. L. A. Vasil'ev, Shadow Methods [in Russian], Nauka, Moscow (1968).